

Lunar Reconnaissance Orbiter K-band (26 GHz) Signal Analysis: Updated Study Results

David D. Morabito* and David Heckman*

ABSTRACT. — Lower frequency telemetry bands are becoming more limited in bandwidth due to increased competition between flight projects and other entities. Higher frequency bands offer significantly more bandwidth and hence the prospect of much higher data return.

Future or prospective flight projects considering higher frequency bands, such as Ka-band (32 GHz) for deep-space and K-band (26 GHz) for near-Earth telemetry links, are interested in past flight experience with available received data at these frequencies. Given that there is increased degradation due to the atmosphere at these higher frequencies, there is an effort to retrieve flight data of received signal strength to analyze performance under a variety of factors. This article reports on the analysis of over 11 million observations, collected between near mid-2017 and the beginning of 2020, of received signal strength of the Lunar Reconnaissance Orbiter (LRO) spacecraft. We analyzed these data to characterize link performance over a wide range of weather conditions, seasons, and as a function of elevation angle. Based on this analysis, we have confirmed the safety of using a 3 dB margin for preflight planning purposes. The results suggest that a 3 dB margin with respect to adverse conditions will ensure a ~98 to 99% data return under 95% weather conditions at 26 GHz, thus confirming the expectations from link budget predictions. The results of this study and a previous study suggest that this margin should be applicable for all elevation angles above 10 deg. Thus, missions that have sufficient power for their desired data rates may opt to use 10 deg as their minimum elevation angle. The limitations of this study include climate variability and observations that require removal of hotbody noise in order to perform an adequate cumulative distribution function (CDF) analysis. Flight projects may use other link margins depending upon available information, uncertainties of non-atmospheric link parameters, and mission phase.

I. Introduction

Ka-band (32 GHz) and K-band (26 GHz) offer several advantages for received downlink telemetry and navigation over lower frequency bands, such as wider spectrum allocation, higher antenna gain, and greater immunity to plasma effects. These advantages allow for

* Communications Architectures and Research Section.

increased performance and greater accuracy for navigation data types. Early deep-space Ka-band (32 GHz) experiments and demonstrations include Mars Observer, Mars Global Surveyor, Deep Space 1, and Mars Reconnaissance Orbiter (MRO). More recent deep-space Ka-band flights include Cassini [1] and Kepler [2]. A detailed study of MRO's signal strength data is reported on in reference [3], which also summarizes all of the deep-space Ka-band (32 GHz) statistics from references [1,2,3].

Lunar Reconnaissance Orbiter (LRO) has been orbiting the Moon in a polar orbit since 2009, performing detailed mapping of the lunar surface as well as conducting other measurements. The spacecraft was launched on June 18, 2009, and entered lunar orbit on June 23, 2009. This article reports on the status of received signal data processing from the White Sands 18 m diameter station (designated WS1), focusing on the 26 GHz near-Earth K-band allocation used for high-rate science data downlink. An initial study was previously conducted on the LRO signal strength measurement acquired from 2014-356 (year-day of year) to 2017-229 [4]. This follow-up study reports on signal strength measurement data acquired since the initial study (2017-229) to shortly after the start of 2020 (2020-039), and analyzes over 11 million observations. Based on this current analysis, we found that over 99% of the data points lie above a curve defined 3 dB below the adverse link margin curve.

II. Observations

LRO orbits the Moon in a ~50 km altitude, near-circular orbit with a ~2 hr period. About six tracking passes, each with a duration of ~1 hr, per day are conducted using the 18 m White Sands antenna. LRO has an S-band link (2.2 GHz) used primarily for low-rate engineering data and a K-band link (25.65 GHz) used for high-rate science data. The K-band system has a 40 W transmitter and a 75 cm diameter high-gain dish antenna that provides a downlink consisting of high-rate telemetry data at 100 Mbps in two orthogonal channels of 50 Mbps each. We obtained the nominal values for parameters used in the link budget analysis for the LRO spacecraft and for the White Sands ground station from reference [5].

The models used for atmospheric statistics in the link budgets are based on International Telecommunication Union (ITU) models ([6], and references therein), as well as the weather statistics input to the ITU models. The atmospheric model used in the favorable link budget calculations assumed 50% availability, while the atmospheric model used in the adverse link budget calculations assumed 95% availability.

The lunar hotbody contribution to the system noise temperature used in link calculations was derived from lunar brightness temperature maps at several lunar phase values at 26 GHz [7]. The disk-center values of lunar brightness temperature vary as a function of lunar phase angle. The conversion of brightness temperature to its contribution to system noise temperature uses models provided by reference [7]. For the adverse link budget calculations, we assumed a maximum brightness temperature of 275 K, applicable when LRO is near the lunar disk center (such as during a diametric crossing). For the favorable link budget calculations, we assumed a brightness noise temperature of about 42% of this value, applicable when LRO is near the lunar limb (such as during a grazing orbit). This assumption makes use of a comparison of disk-centered and limb-centered measurements performed at similar frequency and antenna size [7-8].

The range distance between White Sands and the LRO spacecraft over the ~5 yr observation period varied with a monthly periodicity, as shown in Figure 1. The minimum range distance used in the favorable link budget calculations was 352,716 km and the maximum range distance used in the adverse link budget calculations was 412,754 km. This contributes to a 1.37 dB spread in received signal strength between nearest and farthest range distances, which is reflected in the plots showing the raw observations of received E_b/N_0 at White Sands. The minimum range distance between White Sands and LRO on May 27, 2017 coincided within a day of the minimum Earth–Moon distance over this period.

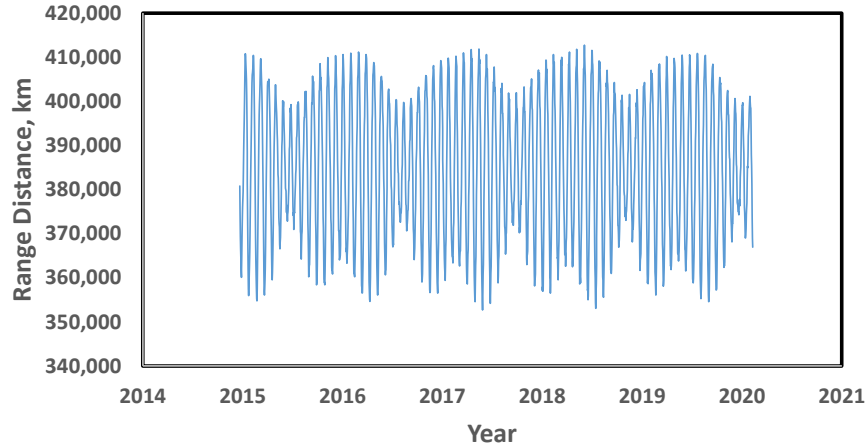


Figure 1. LRO to White Sands range distance.

We started receiving regular data deliveries from the LRO project on year 2016 on day of year 161 (2016-161) after the completion of each tracking pass. A discussion of the earlier data deliveries can be found in reference [4]. Thus, the primary data set includes data acquired from mid-2015 to about mid-2017 for the initial study reported in reference [4].

For these studies, we chose the energy-to-noise ratio per unit bit E_b/N_0 as the signal strength parameter in which to characterize the performance of the link. For a discussion on how lunar hotbody noise temperature varies with lunar phase angle and with orbit type (whether diametric crossing or face-on), see the discussion in reference [4]. The two-week periodicity between face-on and disk-center crossing orbits results in ~2 dB peak-to-peak variation in average E_b/N_0 due primarily to the different contributions of hotbody noise and range distance.

III. Analysis of Individual E_b/N_0 Observations

It is important to analyze the individual sampled observations of received signal strength, so that their statistical significance can be assessed. The individual E_b/N_0 measurements were sampled at 1 s time resolution, resulting in ~3600 data points for each ~1 hr tracking pass. Approximately six tracking passes per day over the course of the several-year period resulted in over 11 million observations (after removing obviously erroneous data points). Due to the amount of observations, we examined them in batches (Figures 2 through 16 display these results for each batch). These plots display the individual E_b/N_0

measurements (blue dots) as a function of elevation angle for each batch of data processed. It is emphasized that no attempt was made to adjust the individual E_b/N_0 measurements for any differences in link parameters in order to preserve the originality of the data. Instead, we compare the measurements with adverse and favorable link assumptions by overlaying these plots with the appropriate curves. Therefore, we plotted the adverse (red curve) and favorable (black curve) link budget curves in Figures 2 through 16. The dashed yellow curves on each plot represent the 3 dB margin curve lying below the adverse curves. For a discussion of the link assumptions built into these curves, the reader is referred to the discussion presented in reference [4].

Table 1 summarizes the previous results reported in reference [4]. Table 2 summarizes the new results, which are plotted in Figures 2 through 16. Tables 1 and 2 display the start and stop dates (first and second columns) for each batch of data displayed in the plots along with the total number of observations (third column) and the number of observations lying above the dashed yellow 3 dB curves (fourth column). The fifth column displays the percentage of data lying above the 3 dB curves for each batch of data. We see that for all cases more than 98% of the data lies above the 3 dB curves. The bottom row summarizes the overall statistical comparison, where 99.2% of the data, consisting of over 10 million observations, lies above the 3 dB curves.

Table 1. LRO E_b/N_0 observation statistics from reference [4].

Start Year-Day	End Year-Day	Number of Data Points	Number of Points >3 dB Curve	Percent >3 dB Curve
2014-356	2014-358	37873	37808	99.83
2015-162	2015-181	323484	321848	99.49
2015-182	2015-212	456029	452480	99.22
2015-213	2015-243	477671	474381	99.31
2015-244	2015-273	444294	442073	99.50
2015-274	2015-304	456456	449285	98.43
2015-305	2015-334	423278	421441	99.57
2015-335	2015-365	405961	403829	99.47
2016-001	2016-031	405129	401928	99.21
2016-032	2016-060	385177	383440	99.55
2016-061	2016-091	414459	413296	99.72
2016-092	2016-121	410079	408439	99.60
2016-122	2016-146	353394	350796	99.26
2016-161	2016-219	707538	702600	99.30
2016-219	2016-277	672197	664049	98.79
2016-277	2016-330	718719	714964	99.48
2016-331	2017-020	679465	669964	98.60
2017-021	2017-073	675049	670357	99.30
2017-074	2017-128	712037	708782	99.54
2017-129	2017-183	696930	693105	99.45
2017-183	2017-229	548142	539454	98.42
Totals		10403361	10324319	99.24

Table 2. LRO E_b/N_0 observation statistics (this study).

Start Year-Day	End Year-Day	Number of Data Points	Number of Points >3 dB Curve	Percent >3 dB Curve
2017-229	2017-284	679596	669839	98.56
2017-285	2017-339	699816	697310	99.64
2017-339	2018-034	755654	752055	99.52
2018-034	2018-102	842246	832070	98.79
2018-102	2018-161	811855	809154	99.67
2018-162	2018-221	822982	814131	98.92
2018-221	2018-280	809747	806438	99.59
2018-281	2018-340	803835	785572	97.73
2018-340	2019-038	798485	793869	99.42
2019-039	2019-099	822361	818742	99.56
2019-099	2019-161	854778	850218	99.47
2019-161	2019-228	842035	831273	98.72
2019-228	2019-292	848266	842314	99.30
2019-292	2019-355	830680	822191	98.98
2019-355	2020-039	628947	625688	99.48
Totals		11851283	11750864	99.15

The black solid curves in Figures 2 through 16 represent the E_b/N_0 versus elevation angle dependence based on favorable link assumptions, which include minimum range distance, minimal hotbody noise (face-on orbits), and nominal atmospheric conditions (50% availability).

Note that these curves do a generally good job of bounding the upper envelope of the E_b/N_0 data points, although based on statistical expectations, we expected a certain percentage of points to lie above the favorable curve. We suspect that there may be a small elevation dependence of the ground antenna gain in vacuum conditions, but a model for this was not available. Such a model may cause the link curves to bend down slightly below the favorable curves at higher elevation angles.

The red solid curves in Figures 2 through 16 represent the E_b/N_0 versus elevation angle dependence based on adverse link assumptions, which include maximum range distance, maximum hotbody noise (disk-center crossing orbit), and adverse atmospheric conditions (95% availability). Note that these curves do a good job of bounding almost all the E_b/N_0 data points falling near the bottom of the main ~2 dB extent of the envelope of the raw observations up to the favorable link curve, corresponding to the limits of hotbody noise, atmospheric loss, and range distance.

The dashed yellow curve represents the link corresponding to 3 dB below the adverse curve. Table 2 itemizes the number of data points and percentage of them that lie above this curve for each batch of data. It should be noted that the adverse - 3 dB curve corresponds to a percent weather availability somewhat greater than 99%. This means that if all other link budget parameters were known with great certainty, then only atmospheric effects would dominate and that less than 1% of the points would fall below this curve,

which is close to what we observed. Table 3 summarizes the results of both studies, where we see similar results were obtained (better than 99%) over a total of more than 22 million observations.

Table 3. LRO E_b/N_0 observation statistics from both studies.

Start Year-Day	End Year-Day	Number of Data Points	Number of Points >3 dB Curve	Percent >3 dB Curve	Comment
2014-356	2017-229	10403361	10324319	99.24	From ref. [4]
2017-229	2020-039	11851283	11750864	99.15	Current study
Overall		22254644	22075183	99.19	Overall

The blue E_b/N_0 data points in Figures 2 through 16 that lie below the dashed yellow curves fall into two main categories.

First, the data points that appear to be connected show trends are more likely due to atmospheric-induced fade features or antenna (either spacecraft or ground) off-pointing signatures not yet removed from the data sets. Non-atmospheric-induced signatures remaining in the data sets would be expected to be identified and removed, but their removal is not expected to significantly change the numerical conclusions.

Second, the data points that appear scattered below the dashed yellow curve and not connected are likely due to periods of high winds, during maneuvers, during signal acquisition at the start of a track, or during loss of signal at the end of a track. These are more difficult to delete as they would require removal by hand, an intense editing process.

In any event, approximately 99% of the data points lie above this curve and removal of non-weather-related events is not expected to significantly change the statistics or the general conclusions. Thus, if we were able to identify such trends as due to non-atmospheric effects and remove them, the statistical results would be better than what we observe (and still >99%).

The percentage of data points lying above the adverse - 3 dB curve is similar from batch to batch, generally running at the 98 to 99% levels, as shown in Table 2. We analyzed a total of 11,851,283 data points, of which 11,750,864 lie above the adverse - 3 dB curve (99.2%).

The E_b/N_0 measurements plotted in Figures 2 through 16 are the raw measurements reported by the receiver. No adjustments were made to the E_b/N_0 data in range distance, weather, or hotbody noise. We had tested a model in which a coarse hotbody noise contribution is removed from the E_b/N_0 measurements [4]. This adjustment tends to reduce the spread (or envelope) of the measurements as expected, but we prefer to report on the raw measurements in this article.

It is noteworthy to point out that all of the available data in this study occurs at elevation angles above 20 deg (Figures 2 through 16) with the exception of one pass in Figure 7 that included elevation angles below 20 deg. The initial study [4] included a significant amount of data that involved a minimum elevation angle of 10 deg. Another noteworthy point is that given that the rainiest months at the White Sands site are July, August, and

September,¹ this correlates well with the plots that show the greatest prevalence of connected features (several likely rain fade features) lying below the adverse red curves in Figures 2 through 16 (specifically Figures 2, 7–8, and 13–14). Periods when there are few or a dearth of such features lying outside of the July–September rainy period include those shown in Figures 3–6, 10–12, and 15–16. One exception is Figure 9, which displays data outside of the rainy period and shows a surprising number of such events, several of which may be due to other contributors, such as antenna mispointing. The removal of any non-atmospheric features in Figures 2 through 16, as well as removal of spurious pre-acquisition and post-track data in these figures, will result in higher percentages of data lying above the 3 dB dashed yellow curves, which are already at the 98 to 99% level. Thus, we could consider the present results to be on the conservative side.

In our initial study, we found high correlation of significant rain-induced events, such as with nearby rain gauge data [4], and high correlation of wind-induced event signatures with wind data from a sensor located near the WS1 antenna [4].

Many of the scattered data points (non-connected features) appearing below the adverse and adverse – 3 dB curves in Figures 2 through 16 are attributable to wind-induced effects on the mechanical structure of the ground antenna. High winds will tend to induce pointing variations, which in turn cause degradation in received signal strength and result in lower E_b/N_0 measurements. When wind speeds are relatively low, the E_b/N_0 measurements exhibit very little scatter. For tracks where the wind speeds approach, and at times, exceed 40 mph, there is appreciable scatter in the E_b/N_0 measurements lying below the adverse link curves. The LRO link documentation [5] specifies a pointing loss of “up to 2 dB” due to wind, but evidently, it can exceed this based on the results of this analysis. Similar behavior has also been observed on deep-space Ka-band (32 GHz) signal data at a 34 m diameter antenna during high winds [2].

After conducting similar examinations of much of the data lying below the adverse – 3 dB curves in Figures 2 through 16, we find that many of the “stringy” connected-point signatures appear correlated with periods of significant rainfall, and many of the scattered points appear correlated with periods of high winds. We therefore conclude that much of the observed degradation in E_b/N_0 data lying below the adverse curves in Figures 2 through 16 are likely atmospheric in nature (both due to moisture and winds). The statistics presented in Table 2 show that ~99% of the E_b/N_0 measurements lie above the adverse – 3 dB curves in Figures 2 through 16. We believe that the subsequent identification and removal of any residual non-atmospheric-induced degraded data (such as slews due to antenna mispointing) would not significantly affect the statistics and, in fact, would increase the percentage of data lying above these curves.

¹ <https://www.nps.gov/whsa/planyourvisit/weather.htm>

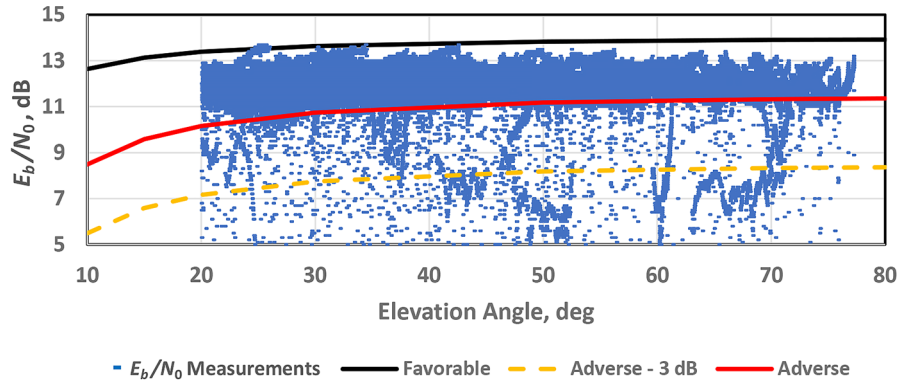


Figure 2. E_b/N_0 vs. Elevation Angle — August 17, 2017 to October 11, 2017 (2017-229 to 2017-284).

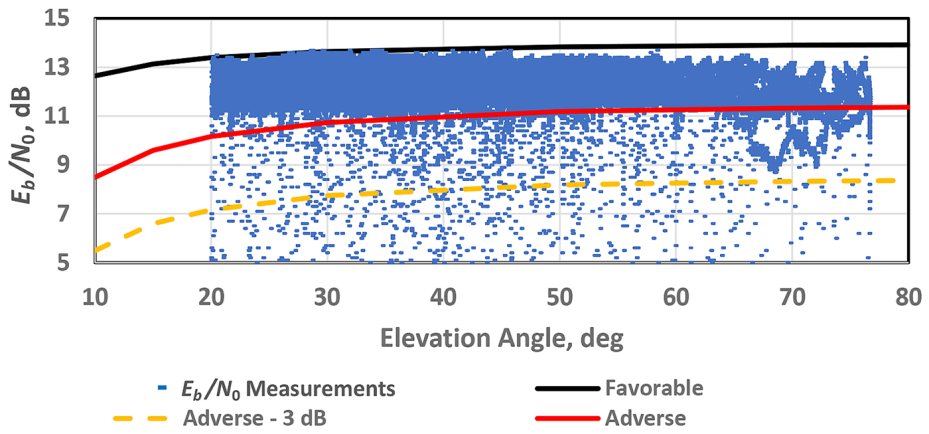


Figure 3. E_b/N_0 vs. Elevation Angle — October 12, 2017 to December 5, 2017 (2017-285 to 2017-339).

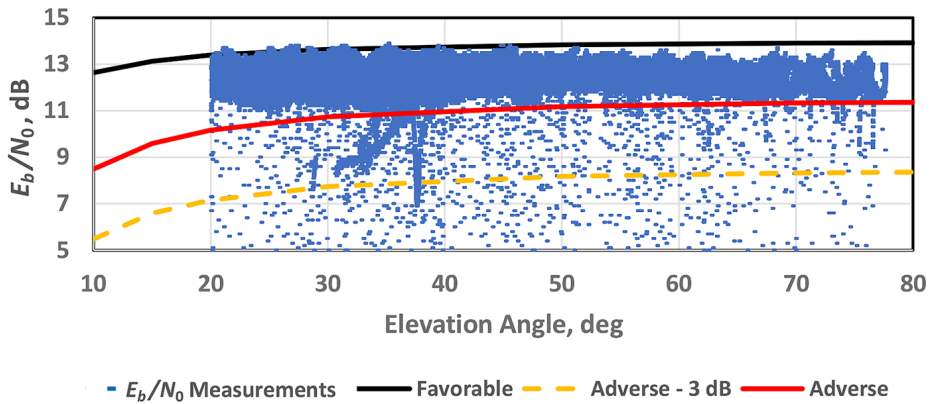


Figure 4. E_b/N_0 vs. Elevation Angle — December 5, 2017 to February 3, 2018 (2017-339 to 2018-034).

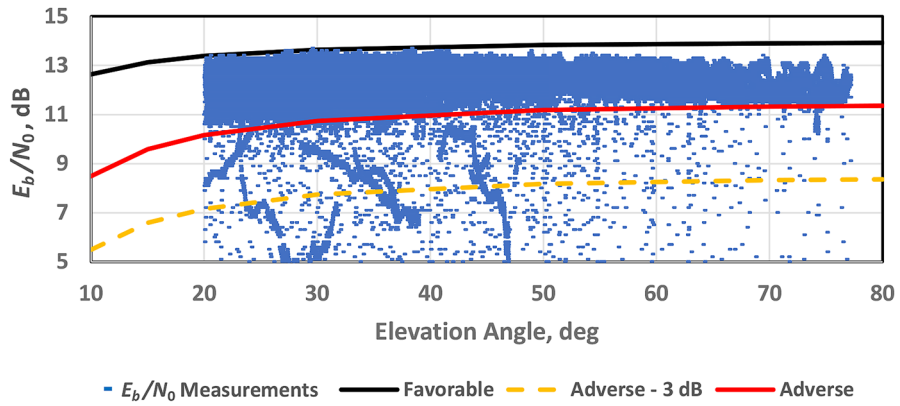


Figure 5. E_b/N_0 vs. Elevation Angle — February 3, 2018 to April 12, 2018 (2018-034 to 2018-102).

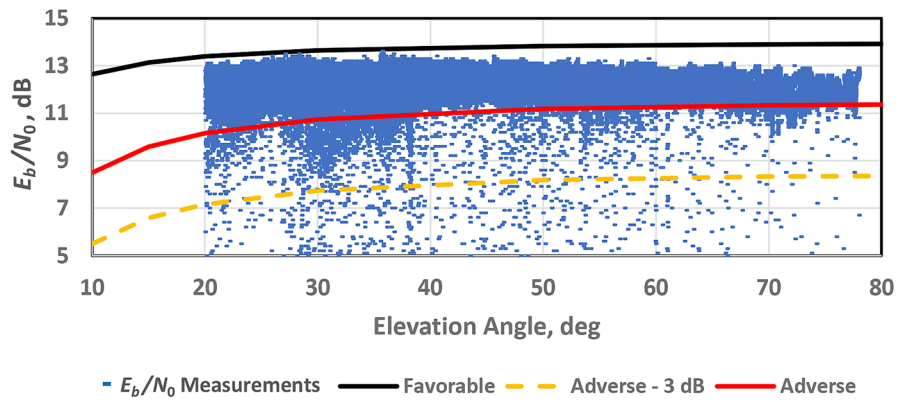


Figure 6. E_b/N_0 vs. Elevation Angle — April 12, 2018 to June 10, 2018 (2018-102 to 2018-161).

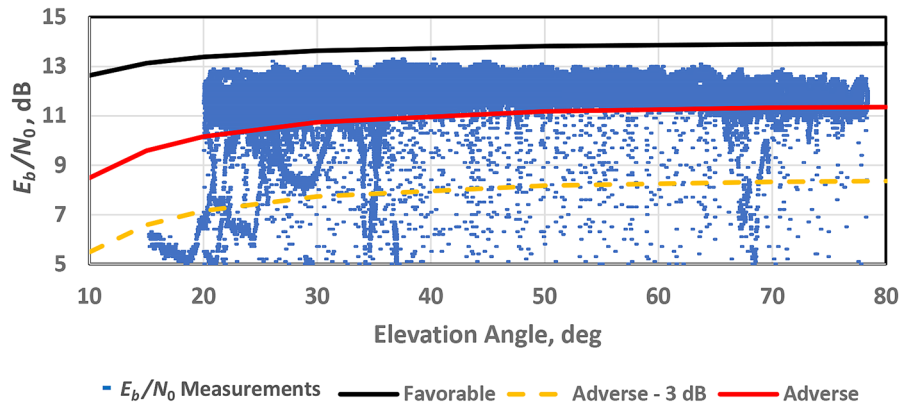


Figure 7. E_b/N_0 vs. Elevation Angle — June 11, 2018 to August 9, 2018 (2018-162 to 2018-221).

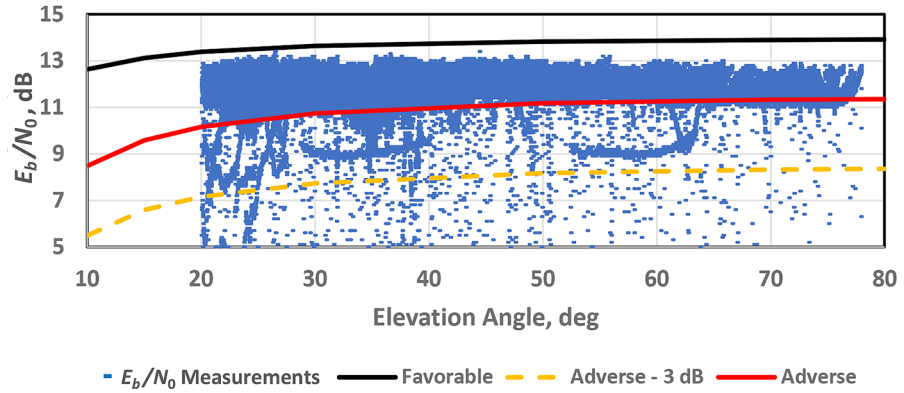


Figure 8. E_b/N_0 vs. Elevation Angle — August 9, 2018 to October 7, 2018 (2018-221 to 2018-280).

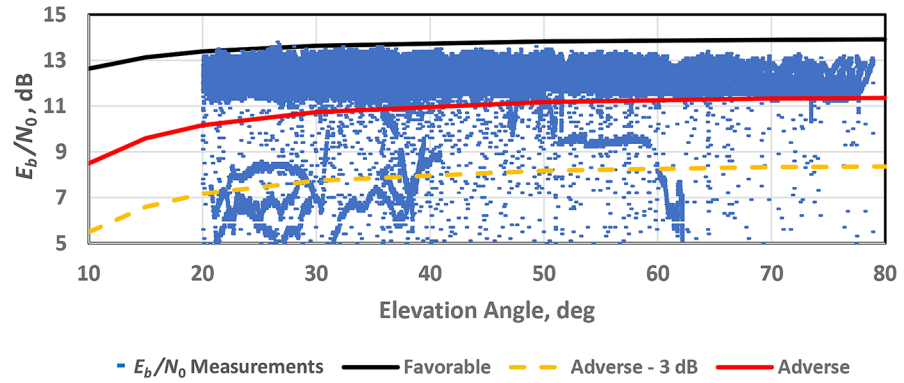


Figure 9. E_b/N_0 vs. Elevation Angle — October 8, 2018 to December 6, 2018 (2018-281 to 2018-340).

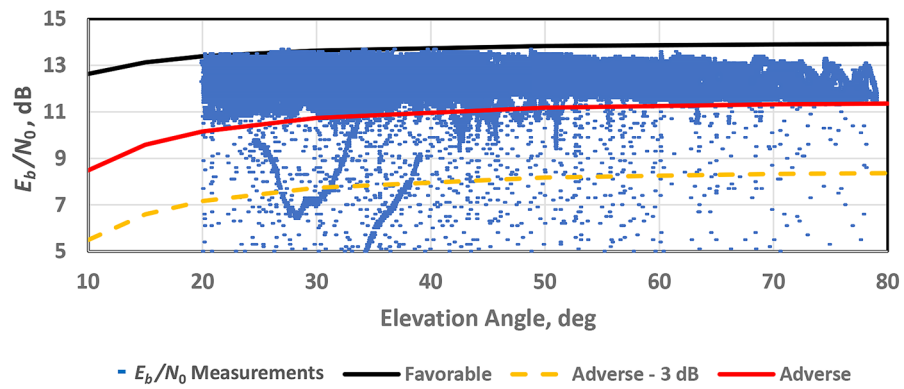


Figure 10. E_b/N_0 vs. Elevation Angle — December 6, 2018 to February 7, 2019 (2018-340 to 2019-038).

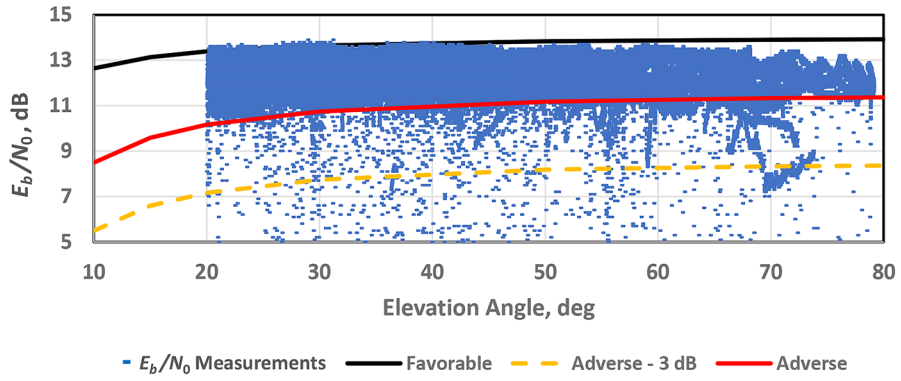


Figure 11. E_b/N_0 vs. Elevation Angle — February 8, 2019 to April 9, 2019 (2019-039 to 2019-099).

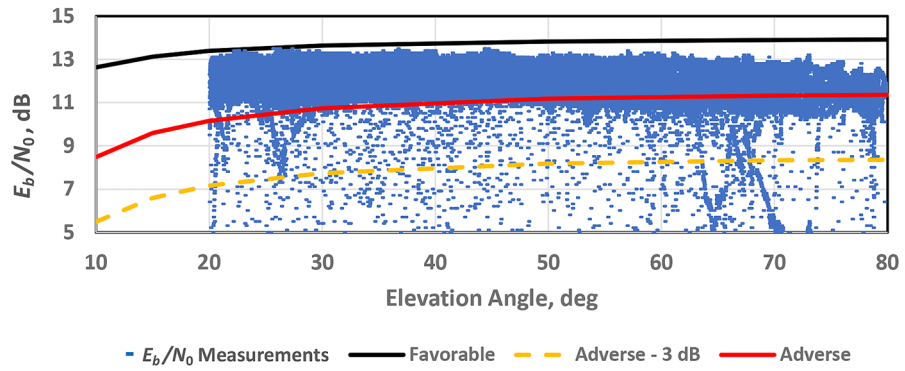


Figure 12. E_b/N_0 vs. Elevation Angle — April 9, 2019 to June 10, 2019 (2019-099 to 2019-161).

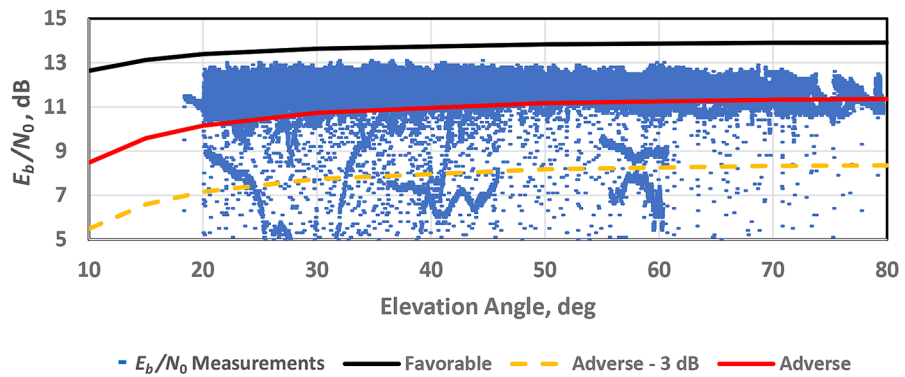


Figure 13. E_b/N_0 vs. Elevation Angle — June 10, 2019 to August 18, 2019 (2019-161 to 2019-228).

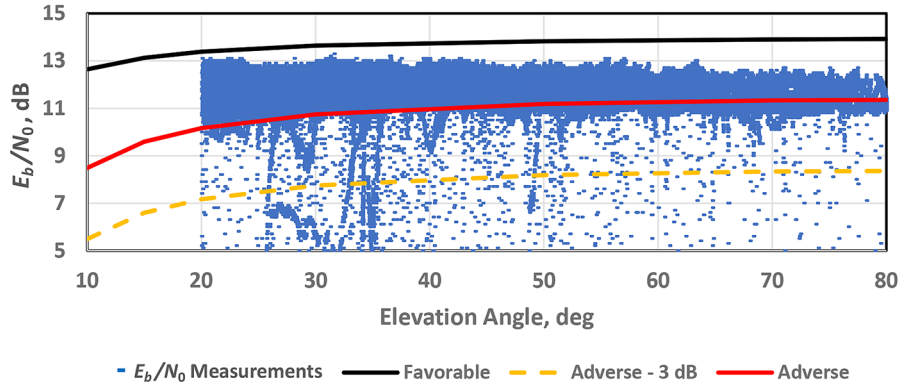


Figure 14. E_b/N_0 vs. Elevation Angle — August 18, 2019 to October 19, 2019 (2019-228 to 2019-292).

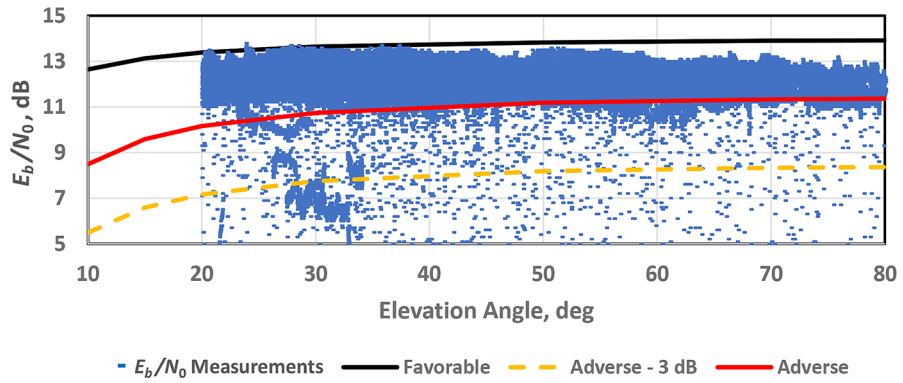


Figure 15. E_b/N_0 vs. Elevation Angle — October 19, 2019 to December 21, 2019 (2019-292 to 2019-355).

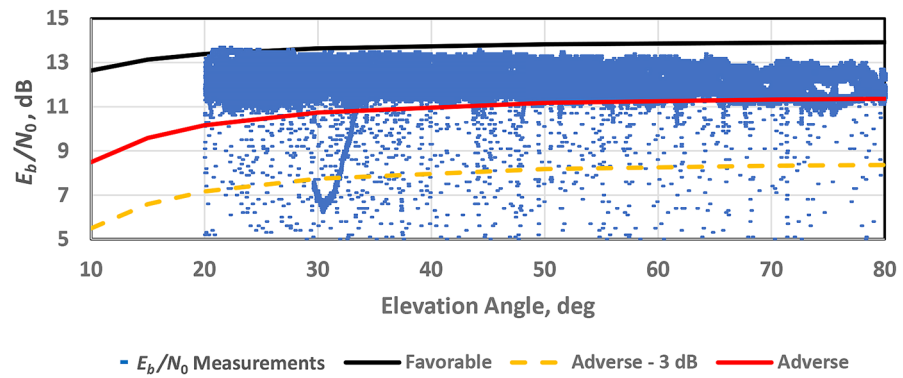


Figure 16. E_b/N_0 vs. Elevation Angle — December 21, 2019 to February 8, 2020 (2019-355 to 2020-039).

Data continuity is not the only value considered by flight projects, as some also value data volume. A CDF analysis would yield a recommendation on what margin to use for best data volume. This present study is limited by the lack of a data volume analysis. Prediction of data volume return as a function of orbit projection at lower frequency bands for

LRO-type missions, accounting for hotbody noise signatures, was the subject of a previous study [9].

Although the favorable and adverse curves do a reasonable job of bounding the main envelope defined by the E_b/N_0 observations versus elevation angle, they do not agree fully with statistical expectations. For example, we expected more observations to lie above the favorable curve in certain cases. This will be the focus of a possible future study when all observations can be adjusted to a common range distance, with removal of hotbody noise contribution and further data editing to remove any non-atmospheric features.

IV. Conclusion

This article reports the findings of analysis of over 11 million observations of received signal strength from the LRO spacecraft collected between 2017 and 2020 at White Sands. These results were found to be consistent with those of the previous study, which reported on ~10 million observations conducted between 2014 and 2017. We analyzed these data to characterize link performance over a wide range of weather conditions, seasons, and as a function of elevation angle. These results show that a 3 dB margin, with respect to adverse link budget assumptions, will ensure a ~99% data return under 95% percent weather conditions at 26 GHz (K-band), thus confirming expectations from link budget predictions. We found that the 3 dB margin is applicable over elevation angles at 10 deg and above. Thus, missions that have sufficient power for their desired data rates may opt to use 10 deg as their minimum elevation angle. The limitations of this study include climate variability and observations that require removal of hotbody noise in order to perform an adequate CDF analysis. Flight projects may use other link margins depending upon available information, uncertainties of non-atmospheric link parameters, and mission phase.

Upcoming missions, such as NASA-ISRO Synthetic Aperture Radar (NISAR) and Plankton, Aerosol, Cloud, ocean Ecosystem (PACE), will be downlinking K-band signals to high-latitude ground terminals whose climates are more amenable to K-band signals. The antenna structures will be enclosed inside radomes to protect against the impact of wind. Work is in progress to install K-band network equipment to support these missions. The ground supports will be baselined to a minimum elevation angle of 10 deg and the link design will include atmospheric based on the current ITU models for those specific locations. Signal strength measurements will be acquired in a similar manner as done for LRO, such that atmospheric degradation can be compared to that estimated from ITU models and data down to a 10 deg elevation angle. NASA Glenn Research Center is also planning on installing a measurement system at the Alaska antenna site to further validate the ITU model data.²

² Frank Stocklin, Goddard Space Flight Center, personnel communication, July 2020.

Acknowledgments

We thank Dimitri Antsos for support of this work. We thank Frank Stocklin for his review of earlier drafts of this article. We acknowledge the assistance of Ralph Casasanta of NASA Goddard Space Flight Center LRO Ground Station and Operation and Engineering Support for arranging the delivery of the data sets and for promptly addressing questions as they arose. We acknowledge Harvey Elliott (Space Communications Network Services Software Engineer at NASA Wallops Flight Facility) for his assistance in recovering and delivering archived data sets and promptly addressing questions as they arose.

References

- [1] D. D. Morabito, D. Kahan, K. Oudrhiri, and C.-A. Lee, "Cassini Downlink Ka-Band Carrier Signal Analysis," *The Interplanetary Network Progress Report*, vol. 42-208, Jet Propulsion Laboratory, Pasadena, California, pp. 1–22, February 15, 2017. http://ipnpr.jpl.nasa.gov/progress_report/42-208/208B.pdf
- [2] D. D. Morabito, "Deep Space Ka-Band Flight Experience," *The Interplanetary Network Progress Report*, vol. 42-211, Jet Propulsion Laboratory, Pasadena, California, pp. 1–16, November 15, 2017. http://ipnpr.jpl.nasa.gov/progress_report/42-211/211B.pdf
- [3] David D. Morabito. Mars Reconnaissance Orbiter Ka-Band Carrier Signal Analysis. *The Interplanetary Network Progress Report*, Volume 42-214, pp. 1–16, August 15, 2018. https://ipnpr.jpl.nasa.gov/progress_report/42-214/42-214B.pdf
- [4] David D. Morabito and David Heckman. Lunar Reconnaissance Orbiter K-Band (26 GHz) Signal Analysis: Initial Study Results. *The Interplanetary Network Progress Report*, Volume 42-211, November 15, 2017. https://ipnpr.jpl.nasa.gov/progress_report/42-211/211A.pdf
- [5] Radio Frequency Interface Control Document (RFICD) Between Lunar Reconnaissance Orbiter (LRO) and the Near-Earth Network (NEN), Deep Space Network (DSN), and Space Network (SN), Revision 1, 450-RFICD-LRO/NEN/DSN/SN, NASA Goddard Space Flight Center, Greenbelt, Maryland, Publication Date: February 2009, Expiration Date: February 2014.
- [6] D. D. Morabito, "A Comparison of Estimates of Atmospheric Effects on Signal Propagation Using ITU Models: Initial Study Results," *The Interplanetary Network Progress Report*, vol. 42-199, Jet Propulsion Laboratory, Pasadena, California, pp. 1–24, November 15, 2014. http://ipnpr.jpl.nasa.gov/progress_report/42-199/199D.pdf
- [7] C. Ho, A. Kantak, S. Slobin, and D. Morabito, "Link Analysis of a Telecommunication System on Earth, in Geostationary Orbit, and at the Moon: Atmospheric Attenuation and Noise Temperature Effects," *The Interplanetary Network Progress Report*, vol. 42-168, Jet Propulsion Laboratory, Pasadena, California, pp. 1–22, February 15, 2007. http://ipnpr.jpl.nasa.gov/progress_report/42-168/168E.pdf

- [8] D. D. Morabito, "Lunar Noise-Temperature Increase Measurements at S-Band, X-Band, and Ka-Band Using a 34-Meter-Diameter Beam-Waveguide Antenna," *The Interplanetary Network Progress Report*, vol. 42-166, Jet Propulsion Laboratory, Pasadena, California, pp. 1-18, August 15, 2006. http://ipnpr.jpl.nasa.gov/progress_report/42-166/166C.pdf
- [9] D. D. Morabito, "Dynamic Telemetry Link Advantage When Tracking a Lunar Orbiter with a 34-m Antenna at 2.3 GHz and 8.4 GHz," *The Interplanetary Network Progress Report*, vol. 42-200, Jet Propulsion Laboratory, Pasadena, California, pp. 1-17, February 15, 2015. http://ipnpr.jpl.nasa.gov/progress_report/42-200/200C.pdf